Computational Sciences and Engineering 1(2) (2021) 123-137

University of Guilan

Computational Sciences and Engineering

journal homepage: https://cse.guilan.ac.ir/

Vibration analysis of fractional viscoelastic CNTs conveying fluid resting on fractional viscoelastic foundation considering nonlocal effects

M. Faraji Oskouie [a] and R. Ansari [a,*]

[a] Faculty of Mechanical Engineering, University of Guilan, P.O. Box 3756, Rasht, Iran.

ARTICLE INFO

Article history:
Available online 30 April 2021

Keywords:

Fractional viscoelastic carbon nanotube
Fluid flow
Fractional viscoelastic foundation
Vibration; Nonlocality

ABSTRACT

Presented herein is an investigation on the vibrational response of fractional viscoelastic carbon nanotubes (CNTs) conveying fluid and resting on a fractional viscoelastic foundation. The CNTs are modeled according to the Euler-Bernoulli beam theory, and the foundation is considered to be Winkler-type. Also, to incorporate the nanoscale effect into the model, Eringen's nonlocal elasticity is applied. Derivation of governing equation is done by a variational principle together with the Kelvin-Voigt viscoelastic model. Two solution approaches are developed for obtaining the time response of embedded fluid-conveying CNTs. The first approach is on the basis of Galerkin's method, while the GDQM and FDM are used in the second approach. Comprehensive numerical results are given to study the effects of elastic foundation, fractional order, damping, fluid, nonlocal parameter, geometrical properties and viscoelasticity coefficient on the time responses of CNTs subject to different boundary conditions.

1. Introduction

Carbon nanotubes (CNTs) since their discovery in 1991 by Iijima [1] have gained great importance in the scope of nanotechnology due to their wide applications [2-8]. CNTs possess excellent thermal, electrical and mechanical properties. In terms of mechanical characteristics, CNTs can resist large strains of up to 10% [9]. Moreover, they are quite flexible and can return to their original shape after bending and buckling [10].

The mechanical behaviors of nanostructures such as bending, buckling and vibration in both linear and nonlinear regimes have been extensively studied in the past two decades. Among the theoretical investigations, continuum models have received considerable popular acclaim. Such popularity may be mainly attributed to the computational efficiency of continuum models when they are compared

* Corresponding author.
E-mail addresses: r_ansari@guilan.ac.ir

http://dx.doi.org/10.22124/cse.2021.19440.1011

to their atomistic counterparts (e.g. MD simulations or DFT calculations). However, the classical continuum models are not appropriate to use at nanoscale since they are not able to capture the size-dependent behavior of nanostructures. Accordingly, several size-dependent continuum theories have been developed up to now.

The surface elasticity theory developed by Gurtin and Murdoch [11, 12] is a size-dependent theory with the capability of considering the surface stress effect. The concept of surface stress in solids was first proposed by Gibbs [13] in the beginning of 20th century. In nanostructures, the surface stress influence is of considerable significance because of large surface-to-volume ratio. There are numerous studies in the literature on the mechanical behaviors of nanoscale structures in which the surface stress effect has been taken into account [14-21].

The nonlocal theory initiated by Eringen [22, 23] is another size-dependent continuum theory applicable to the problems of small-scale systems. In this theory, the nonlocal effects are considered assuming that the stress at a point is a function of strains at all points in the body. A literature review shows that Eringen’s nonlocal theory has been widely applied to the problems of nanostructures including bending [24], buckling [25-29] and vibration [30-35].

Nanotubes can be used in nanofluidic systems. In this regard, fluid storage, fluid transport and drug delivery can be mentioned as the related applications [36-39]. Hence, several research workers have analyzed the mechanical behaviors of nanotubes conveying fluid based on the size-dependent continuum models. For example, Zhang and Meguid [40] utilized the Gurtin-Murdoch theory to study the vibrational characteristics of simply-supported and clamped fluid-conveying nanotubes including the surface stress effect. Ansari et al. [41] investigated the nonlinear free vibrations and instability of fluid-conveying boron nitride nanotubes embedded in thermal environment. They developed a strain gradient Timoshenko beam model to incorporate the effects of transverse shear deformation, rotary inertia and small-scale into the formulation. The influence of longitudinal magnetic field on the transverse vibrations of magnetically sensitive CNTs conveying fluid was analyzed by Hosseini and Sadeghi-Goughari [42] based upon the nonlocal theory. Ansari and his associates [43, 44] studied the linear/nonlinear vibrations and instability of nanopipes conveying fluid using the Timoshenko beam theory. The surface stress effect was also considered according to the Gurtin-Murdoch theory. Chang [45] developed a nonlocal beam model in order to study instability and vibrations of fluid-filled CNTs.

Analysis of viscoelastic nanosystems using the fractional calculus has recently attracted the attention of some researchers (e.g. [46-48]). Ansari et al. [47] developed a fractional nonlocal model for vibration analysis of viscoelastic CNTs based on the Timoshenko beam theory considering the effect of viscoelastic foundation.

In the present paper, the free vibrational behavior of viscoelastic conveying fluid nanotubes considering the effect of elastic foundation is analyzed based on the fractional calculus. Eringen’s nonlocal theory is used for considering the small scale effect. Also, the Kelvin-Voigt model is employed for the viscoelastic behavior. The governing equation of vibrating CNTs conveying fluid is obtained using Hamilton’s principle and Euler-Bernoulli beam model. Two methods are presented for the solution of problem. In the first approach, the Galerkin method is applied for discretizing the spatial variable and reducing the governing PDE to an ordinary differential equation on the time domain. Then, the Simulink toolbar of MATLAB software is used to obtain the time response of CNT. In the second approach which is applicable for CNTs with arbitrary boundary conditions, the

GDQ technique is applied for discretizing the governing equation on spatial grids, and FDM is employed to discretize it on the time domain. In the numerical results, the impacts of important parameters such as fluid flow and elastic foundation on the vibrations of viscoelastic CNTs conveying fluid are illustrated.

2. Governing Equation

Fig. 1 illustrates the schematic view of the problem.

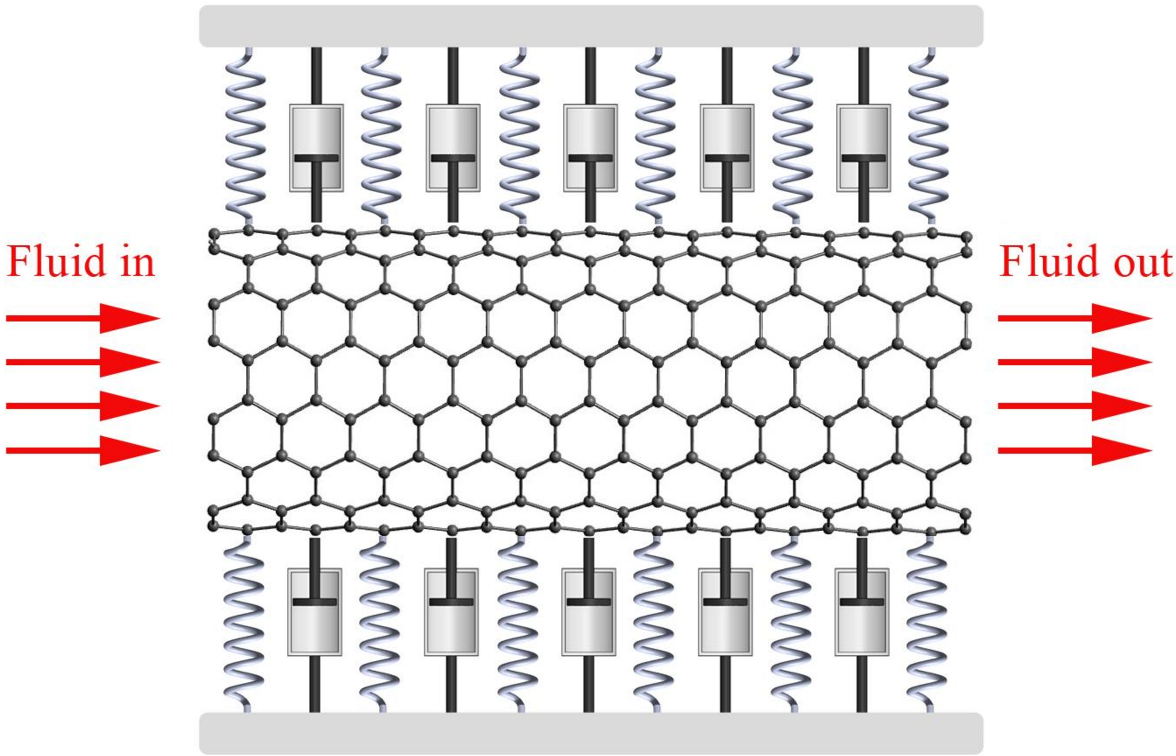

Figure. 1. Schematic of the problem

Based on the Bernoulli-Euler theory, the displacement field is expressed as

$$u_x = u_0(t,x) + z\frac{\partial w_0}{\partial x}, u_y = 0, u_z = w_0(t,x) \tag{1}$$

The strain components are given by

$$\varepsilon_{xx} = \frac{\partial u_0}{\partial x} + z\frac{\partial^2 w_0}{\partial x^2},\ \ \varepsilon_{xz} = \frac{1}{2}\frac{\partial w_0}{\partial x} \tag{2}$$

The total strain energy of the CNT can be also written as

$$\Pi_s = \frac{1}{2}\int_x \left\{ N_{xx}\frac{\partial u_0}{\partial x} + M_{xx}\frac{\partial^2 w_0}{\partial x} \right\} dx \tag{3}$$

in which

$$N_{xx} = \int_A \sigma_{xx} dA\,, \qquad M_{xx} = \int_A \sigma_{xx} z dA \tag{4}$$

The kinetic energy of the CNT is

$$\Pi_T = \frac{1}{2}\int_x \left\{ m \left[\left(\frac{\partial u_0}{\partial t} - z \frac{\partial^2 w_0}{\partial x \partial t} \right)^2 + \left(\frac{\partial w_0}{\partial t} \right)^2 \right] \right\} dx \tag{5}$$

where m is the mass per unit length of the CNT.

Similarly, the kinetic energy of the fluid flow inside the CNT can be formulated as

$$\Pi_f = \frac{1}{2}\int_x \left\{ M \left(\frac{\partial w_0}{\partial t} + U \frac{\partial w_0}{\partial x} \right)^2 + M \left(\frac{\partial u_0}{\partial t} + U \right)^2 \right\} dx \tag{6}$$

where M and U are the mass per unit length and the steady flow velocity of the internal moving fluid, respectively.

Moreover, the work done by the transverse force $q(t,x)$ can be written as

$$\Pi_w = \int_x q(t,x) w_0 dx \tag{7}$$

Hamilton's principle is now applied which is given as

$$\delta \int_{t_1}^{t_2} (\Pi_T + \Pi_f - \Pi_s + \Pi_w) dt = 0 \tag{8}$$

The governing equations are now derived as

$$\frac{\partial N_{xx}}{\partial x} = (M+m) \frac{\partial^2 u_0}{\partial t^2} \tag{9}$$

$$\begin{aligned} \frac{\partial^2 M_{xx}}{\partial x^2} + \frac{\partial}{\partial x}\left(N_{xx} \frac{\partial w}{\partial x} \right) + q \\ = (M+m) \frac{\partial^2 w_0}{\partial t^2} + (M+m) \frac{\partial^2 w_0}{\partial t^2} + 2MU \frac{\partial^2 w_0}{\partial x \partial t} + MU^2 \frac{\partial^2 w_0}{\partial x^2} \end{aligned} \tag{10}$$

where N_{xx} and M_{xx} are resultant axial stress and bending moment, respectively.

The force of the fractional viscoelastic Winkler foundation can be written as

$$q = -k w_0 - c \frac{\partial^\beta w_0}{\partial t^\beta} \tag{11}$$

in which k and c are Winkler's spring and damping modulus, respectively.

Based on Eringen's nonlocal theory and Kelvin-Voigt model [22, 23, 49], the in-plane resultant force and resultant bending moment are expressed as

$$N_{xx} = (e_0 a)^2 \frac{\partial^2 N_{xx}}{\partial x^2} + EA \left(1 + \hat{g} \frac{\partial^\alpha}{\partial \mathrm{t}^\alpha} \right) \frac{\partial u_0}{\partial x}, \tag{12}$$

$$M_{xx} = (e_0 a)^2 \frac{\partial^2 M_{xx}}{\partial x^2} + EI \left(1 + \hat{g} \frac{\partial^\alpha}{\partial \mathrm{t}^\alpha} \right) \frac{\partial^2 w_0}{\partial x^2}, \tag{13}$$

where e_0a is the nonlocal parameter through which the size effects can be captured. By substituting Eqs. (12) and (13) into Eqs. (9) and (10), the explicit expressions of nonlocal in-plane resultant force and resultant bending moment can be achieved as

$$N_{xx} = EA\left(1+\hat{g}\frac{\partial^\alpha}{\partial \mathrm{t}^\alpha}\right)\frac{\partial u_0}{\partial x} - N_T + (e_0a)^2(m+M)\frac{\partial^3 u_0}{\partial x \partial t^2}, \tag{14}$$

$$\begin{aligned} M_{xx} = EI\left(1+\hat{g}\frac{\partial^\alpha}{\partial \mathrm{t}^\alpha}\right)\frac{\partial^2 w_0}{\partial x^2} \\ &+ (e_0a)^2\left[(M+m)\frac{\partial^4 w_0}{\partial x^2 \partial t^2} + 2MU\frac{\partial^4 w_0}{\partial x^3 \partial t} + MU^2\frac{\partial^4 w_0}{\partial x^4}\right. \\ &\left. - \frac{\partial^3}{\partial x^3}\left(N_{xx}\frac{\partial w}{\partial x}\right) - \frac{\partial^2 q}{\partial x^2}\right], \end{aligned} \tag{15}$$

By substituting Eqs. (14) and (15) into (10), the governing equation of the system is obtained as

$$\begin{aligned} EI\left(1+\hat{g}\frac{\partial^\alpha}{\partial \mathrm{t}^\alpha}\right)\frac{\partial^4 w_0}{\partial x^4} + \{MU^2+PA-T^*\}\frac{\partial^2 w_0}{\partial x^2} + 2MU\frac{\partial^2 w_0}{\partial x \partial t} + \mathrm{kw}_0 + \mathrm{c}\frac{\partial^\beta w_0}{\partial t^\beta} \\ &+ (M+m)\frac{\partial^2 w_0}{\partial t^2} \\ &- (e_0a)^2\left[\{MU^2+PA-T^*\}\frac{\partial^4 w_0}{\partial x^4} + 2MU\frac{\partial^4 w_0}{\partial x^3 \partial t} + +\mathrm{k}\frac{\partial^2 w_0}{\partial x^2}\right. \\ &\left. + \mathrm{c}\frac{\partial^{2+\beta} w_0}{\partial x^2 \partial t^\beta} + (M+m)\frac{\partial^4 w_0}{\partial t^2 \partial x^2}\right] = 0 \end{aligned} \tag{16}$$

where T^* and P are externally applied tension and pressurization influeneces, respectively. As reported in [50] for elastic tubes, regardless of the details of the wall–fluid interaction and the viscosity of the fluid, tension (T^*) and pressure drop (PA) cancel each other out. Considering the following definitions

$$\begin{aligned} w = \frac{w_0}{L}, \quad \Psi = \psi, \quad \xi = \frac{x}{L}, \quad \tau = \frac{t}{L^2}\sqrt{\frac{EI}{M+m}}, \\ &\mu^2 = \frac{(e_0a)^2}{L^2}, \quad g = \frac{\hat{g}}{L^2}\sqrt{\frac{EI}{M+m}}, \quad V = UL\sqrt{M/EI}, \quad \overline{N_T} = \frac{N_T}{EA}, \\ &R = \frac{M}{M+m}, \quad C = \frac{cL}{\sqrt{EA(m_1+m_{1f})}}, \quad K = \frac{kL^4}{EA}, \quad P = \frac{\kappa_s G}{E} \end{aligned} \tag{17}$$

the dimensionless governing equation is derived as

$$\begin{aligned} \left(1+g\frac{\partial^\alpha}{\partial \tau^\alpha}\right)\frac{\partial^4 \mathrm{w}}{\partial \xi^4} - \mathrm{V}^2\frac{\partial^2 \mathrm{w}}{\partial \xi^2} + \mathrm{Kw} + \mathrm{C}\frac{\partial^\beta w}{\partial \tau^\beta} + 2\sqrt{R}V\frac{\partial^2 \mathrm{w}}{\partial \xi \partial \tau} + \frac{\partial^2 \mathrm{w}}{\partial \tau^2} \\ &- \mu^2\left(K\frac{\partial^2 \mathrm{w}}{\partial \xi^2} + \mathrm{C}\frac{\partial^{2+\beta} w}{\partial \xi^2 \partial \tau^\beta} - V^2\frac{\partial^4 \mathrm{w}}{\partial \xi^4} + 2\sqrt{R}V\frac{\partial^4 \mathrm{w}}{\partial \xi^3 \partial \tau} + \frac{\partial^4 \mathrm{w}}{\partial \tau^2 \partial \xi^2}\right) \\ &= 0 \end{aligned} \tag{18}$$

3. Solution Approaches

3.1. First Approach

In this approach, first, the Galerkin method is used for discretizing the spatial variable and reducing the governing PDE to an ODE on the time domain. For the simply supported-simply supported boundary conditions (SS) one can write

$$w(\zeta,T)=\sum_{n=1}^{\infty}\varphi_n(T)\sin(n\pi\zeta) \tag{19}$$

in which $\varphi_n(T)$ indicates the unknown time-dependent coefficient. Also, $\sin(n\pi\zeta)$ stands for the modal functions of linear vibrations corresponding to the vibrations of CNT with SS end conditions.

By the first modal function ($n=1$), the following time-dependent ODE is obtained

$$\begin{aligned}(1+\pi^2\mu^2)\ddot{\varphi}_1+V^2\pi^2(1+\mu^2\pi^2)\varphi_1+\pi^4\left(\varphi_1+g\varphi_1^{(\alpha)}\right)+K(1+\mu^2\pi^2)\varphi_1\\ +C(1+\mu^2\pi^2)\varphi_1^{(\beta)}=0\end{aligned} \tag{20}$$

that can be solved considering initial displacement and velocity [51].

3.2. Second Approach

In the second approach, which is numerical, CNTs with various end conditions can be analyzed. The GDQ is employed for discretizing on spatial grids, and FDM is used for discretizing on the time domain.

3.2.1. GDQ

In this method one has

$$\left.\frac{\partial^r f(x)}{\partial x^r}\right|_{x=x_i}=\sum_{j=1}^{N}\mathcal{W}_{ij}^{(r)}f(x_j) \tag{21}$$

in which [52]

$$\mathcal{W}_{ij}^{(r)}= \tag{22}$$

$$\begin{cases}\mathbf{I}_x,\quad \text{where } \mathbf{I}_x \text{ is a } N\times N \text{ identity matrix}, & r=0\\ \dfrac{\mathcal{P}(x_i)}{(x_i-x_j)\mathcal{P}(x_j)},\text{where } \mathcal{P}(x_i)=\prod_{j=1;\,j\neq i}^{N}(x_i-x_j), & i\neq j \text{ and } i,j=1,\ldots,N\ and\ r=1\\ r\left[\mathcal{W}_{ij}^{(1)}\mathcal{W}_{ii}^{(r-1)}-\dfrac{\mathcal{W}_{ij}^{(r-1)}}{x_i-x_j}\right], & i\neq j \text{ and } i,j=1,\ldots,N\ and\ r=2,3,\ldots N-1\\ -\sum_{j=1;\,j\neq i}^{N}\mathcal{W}_{ij}^{(r)}, & i=j \text{ and } i,j=1,\ldots,N\ and\ r=1,2,3,\ldots N-1\end{cases}$$

By introducing the following column vector

$$\mathbf{F} = [f(x_1) \quad f(x_2) \quad \cdots \quad f(x_N)]^{\mathrm{T}} \tag{23}$$

Eq. (21) can be rewritten as

$$\frac{d^r}{dx^r}\mathbf{F} = \mathbf{D}_x^{(r)}\mathbf{F} \tag{24}$$

where $\mathbf{D}_x^{(r)} = \left[\mathcal{W}_{ij}^{(r)}\right]$ is the operational matrix of differentiation, $i, j = 1, \ldots, N$ and $r = 0,1,2, \ldots, N-1$.

3.2.2. FDM

The fractional derivative of a function is written as [53, 54]

$$\frac{1}{\Gamma(1-\alpha)}\int_0^{t_{k+1}}\frac{w'(t_{k+1}-\tau)}{\tau^{\alpha}}d\tau = \frac{\tau^{\alpha}}{\Gamma(2-\alpha)}\sum_{j=0}^{k} b_j^{\alpha}\left[w(t_{k+1-j}) - w(t_{k-j})\right]$$

$$b_j^{\alpha} = (j+1)^{1-\alpha} - j^{1-\alpha}, \qquad j = 0,1,2,..,n \tag{25}$$

where $0 < \alpha < 1$ denotes the order of fractional derivative.

3.2.3. Discretization

The grid is selected as

$$\zeta_i = \frac{1}{2}\left(1 - \cos\frac{i-1}{n-1}\pi\right), \qquad i = 1,2,3, \ldots, n \tag{26}$$

Also,

$$\tau_i = j\frac{T}{m+1}, \qquad j = 0, 2, 3, \ldots, m \tag{27}$$

By introducing the following matrix

$$\mathbf{W} = \begin{bmatrix} w_{10} & w_{12} & \cdots & w_{1n} \\ w_{20} & \ddots & \ddots & w_{2n} \\ \vdots & \ddots & \ddots & \vdots \\ w_{m0} & w_{m2} & \cdots & w_{mn} \end{bmatrix}, \qquad i = 1..m, \qquad j = 0..n \tag{28}$$

in which $w_{ij} = w(x_i, t_j)$. Based on GDQ and FDM:

$$\left[\mathbf{I}_{\zeta} - \mu^2\mathbf{D}_{\zeta}^2\right]\mathbf{W}\mathbf{D}_{\mathrm{t}}^{2^{\mathrm{T}}} - V^2\left(\mathbf{D}_{\zeta}^2\mathbf{W}\right)\left(\mathbf{I}_t^{\mathrm{T}} + \hat{g}\mathbf{D}_{\mathrm{t}}^{\alpha\mathrm{T}}\right) + K\left[\mathbf{I}_{\zeta} - \mu^2\mathbf{D}_{\zeta}^2\right]\mathbf{W}\mathbf{I}_t^{\mathrm{T}} + C\left[\mathbf{I}_{\zeta} - \mu^2\mathbf{D}_{\zeta}^2\right]\mathbf{W}\mathbf{D}_{\mathrm{t}}^{\beta^{\mathrm{T}}} + 2\sqrt{R}V\left[\mathbf{I}_{\zeta} - \mu^2\mathbf{D}_{\zeta}^2\right]\mathbf{W}\mathbf{D}_{\mathrm{t}}^{1^{\mathrm{T}}} - \hat{g}\left(\frac{1}{\Gamma(1-\alpha)\boldsymbol{t}^{\alpha}}\right) \otimes \left(-\mathrm{V}^2\mathbf{D}_{\zeta}^2\mathbf{W_0}\right)^T - C\left(\frac{1}{\Gamma(1-\beta)\boldsymbol{t}^{\beta}}\right) \otimes \left(\mathbf{I}_{\zeta}\mathbf{W}_0 - \mu^2\mathbf{D}_{\zeta}^2\mathbf{W}_0\right)^T = 0 \tag{29}$$

In Eq. (29), $\mathbf{W_0}$ indicates the initial values of W; $\boldsymbol{t}$ is the vector of time; $\mathbf{I}$ is the identity matrix and $\mathbf{D}_{\mathrm{t}}^{\alpha}$, $\mathbf{D}_{\mathrm{t}}^{\beta}$ are the fractional derivative operators of order α and β.

The mode shape for the vibration of elastic nanotube is considered as the initial displacement. Furthermore, the initial velocity is taken to be zero. By applying the discretized conditions to the governing equation, one can arrive at an algebraic set of equations.

4. Numerical Results

The dimensionless maximum amplitude is plotted against dimensionless time for CNTs under three sets of end conditions including C-C, C-SS and SS-SS conditions. The following parameters are also used [55]:

$$D_o = 100\ nm, \quad h = 10\ nm, \quad \rho_{CNT} = 2.3\ \frac{g}{cm^3}, \quad E = 1\ TPa, \quad \rho_f = 1\ \frac{g}{cm^3}, \quad \nu = 0.2$$

First, a comparison is made in Fig. 2 between the results obtained from the first and second solution methods presented in Section 3. In this figure, the time responses of CNT with SS-SS boundary conditions are shown for different values of fractional derivative orders α and β. The agreement observed between predictions by two approaches can confirm the validity of the results of present study. The influences of fractional derivative orders on the time response of CNT can be also seen in Fig. 2 which will be discussed in the following two figures. From now on, the second approach, that is able to model CNTs with different boundary conditions, is employed to generate the results.

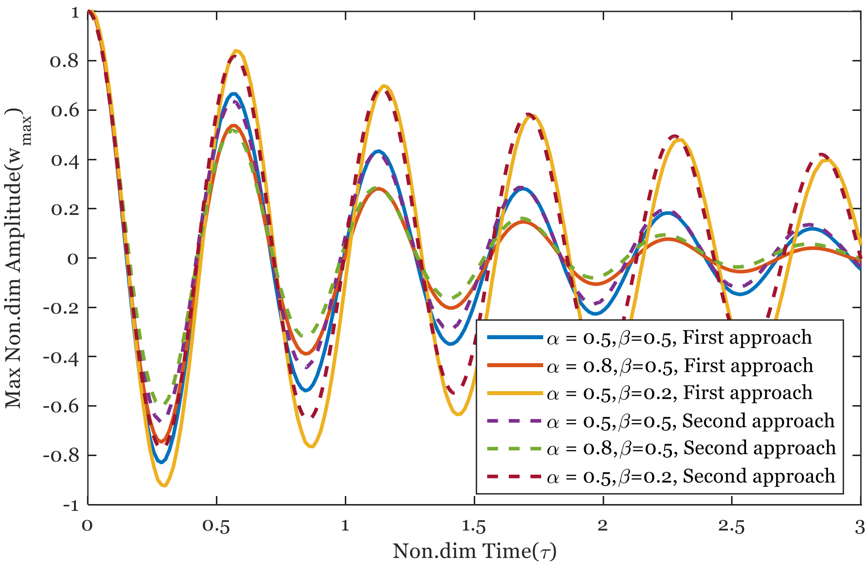

Figure. 2. Comparison between the results of two solution approaches for simply-supported CNT ($\boldsymbol{K = 1\ GPa, V = 100\ \frac{m}{s}, \frac{L}{D_o} = 25, c = 5, \mu = 0.05, g = 0.02}$)

In Fig. 3, the influence of fractional derivative order α, which is related to the structural damping, on the time response of CNTs with SS-SS, C-C and C-SS boundary conditions is investigated. One can find that by increasing α, the frequency of system does not change considerably, but the damping of amplitude is intensified. Fig. 4 also indicates the effect of fractional derivative order β, which is associated with the viscoelastic foundation. It is observed that the effect of β is similar to that of α. Moreover, Figs. 3 and 4 reveal that the behavior of CNT is dependent on the selecetd boundary conditions.

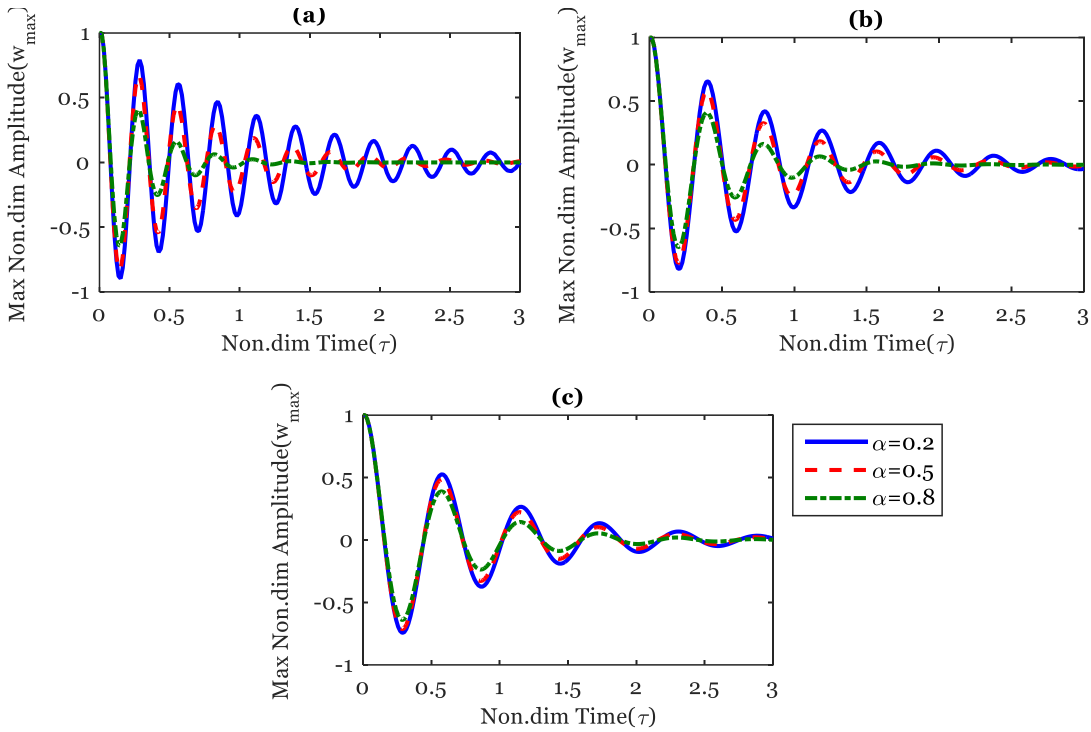

Figure. 3. Effect of $\boldsymbol{\alpha}$ on the time response of nanotube for a) C-C b) C-SS and c) SS-SS boundary conditions ($\boldsymbol{K = 1\ GPa, V = 300\ \frac{m}{s}, \frac{L}{D_o} = 25, c = 10, \mu = 0.1, g = 0.02, \beta = 0.5}$)

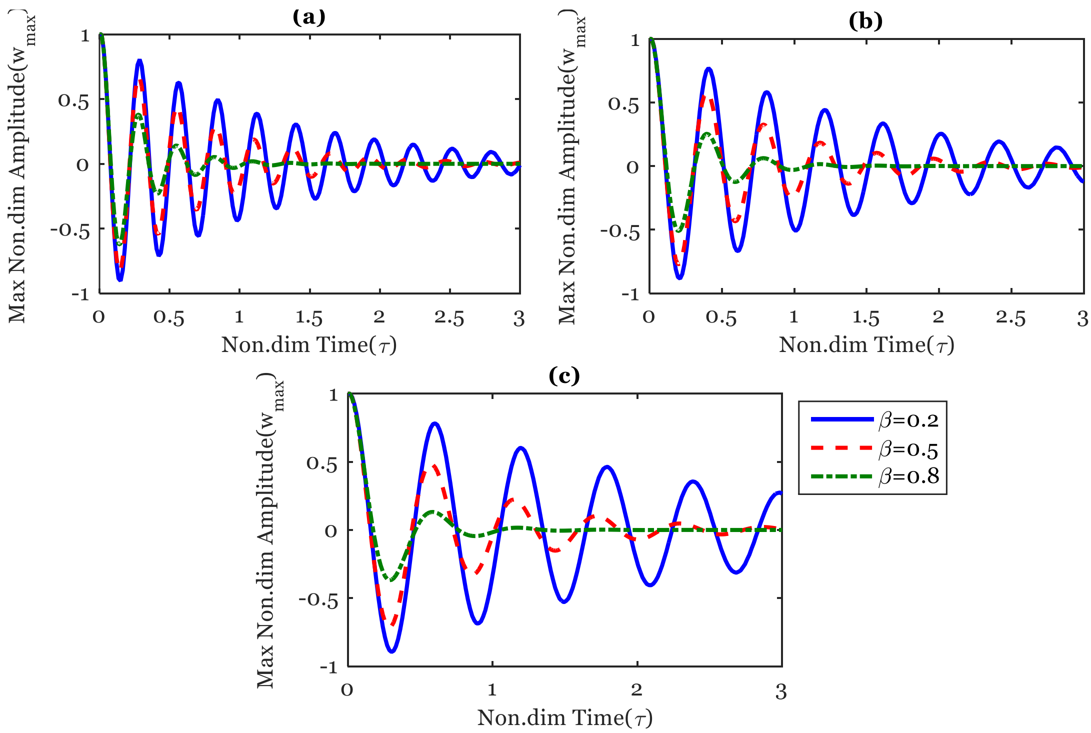

Figure. 4. Effect of $\boldsymbol{\beta}$ on the time response of nanotube for a) C-C b) C-SS and c) SS-SS boundary conditions ($\boldsymbol{K = 1\ GPa, V = 300\ \frac{m}{s}, \frac{L}{D_o} = 25, c = 10, \mu = 0.1, g = 0.02, \alpha = 0.5}$)

Fig. 5 illustrates the time responses of nanotubes for different values of foundation's spring coefficient. The results show that the frequency gets larger as this coefficient increases. In fact, the increase of foundation's spring coefficient leads to the increase of system's stiffness.

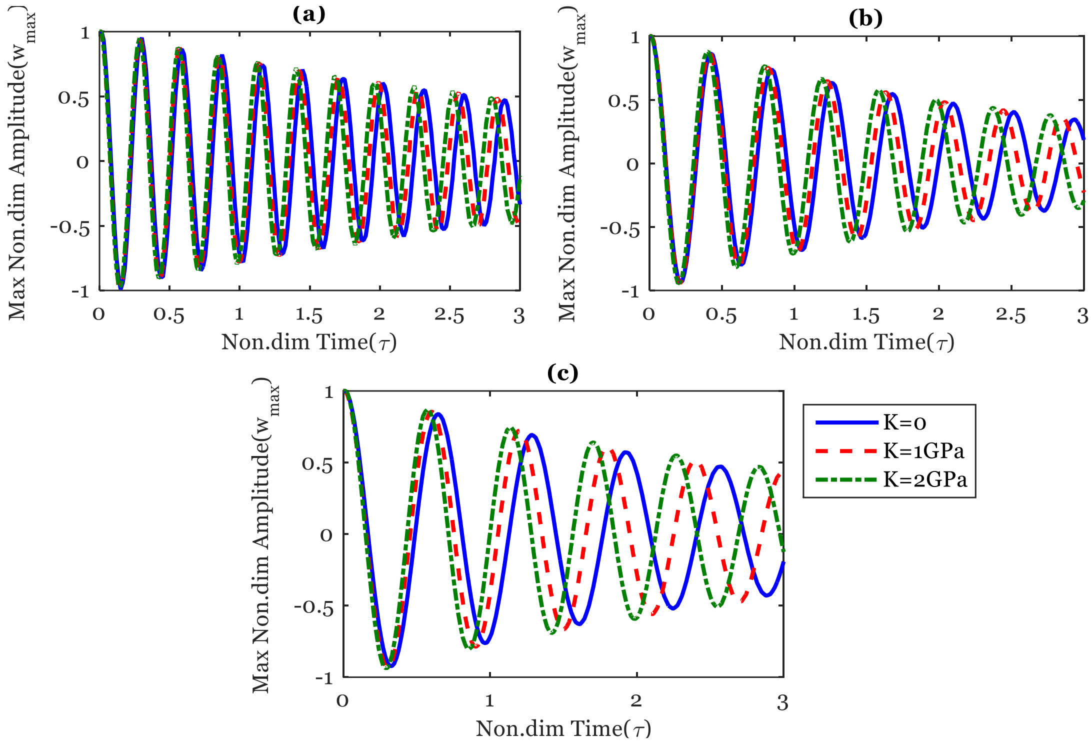

Figure. 5. Effect of foundation's spring coefficient on the time response of nanotube for a) C-C b) C-SS and c) SS-SS boundary conditions ($\boldsymbol{V = 300\ \frac{m}{s}, \frac{L}{D_o} = 25, c = 10, \mu = 0.1, g = 0.02, \alpha = 0.2, \beta = 0.2}$)

The influence of fluid flow velocity on the time response of CNTs is highlighted in Fig. 6. According to this figure, the frequency of system decreases with increasing fluid flow velocity. At higher values of fluid flow velocity, the frequency decreases to a greater extent.

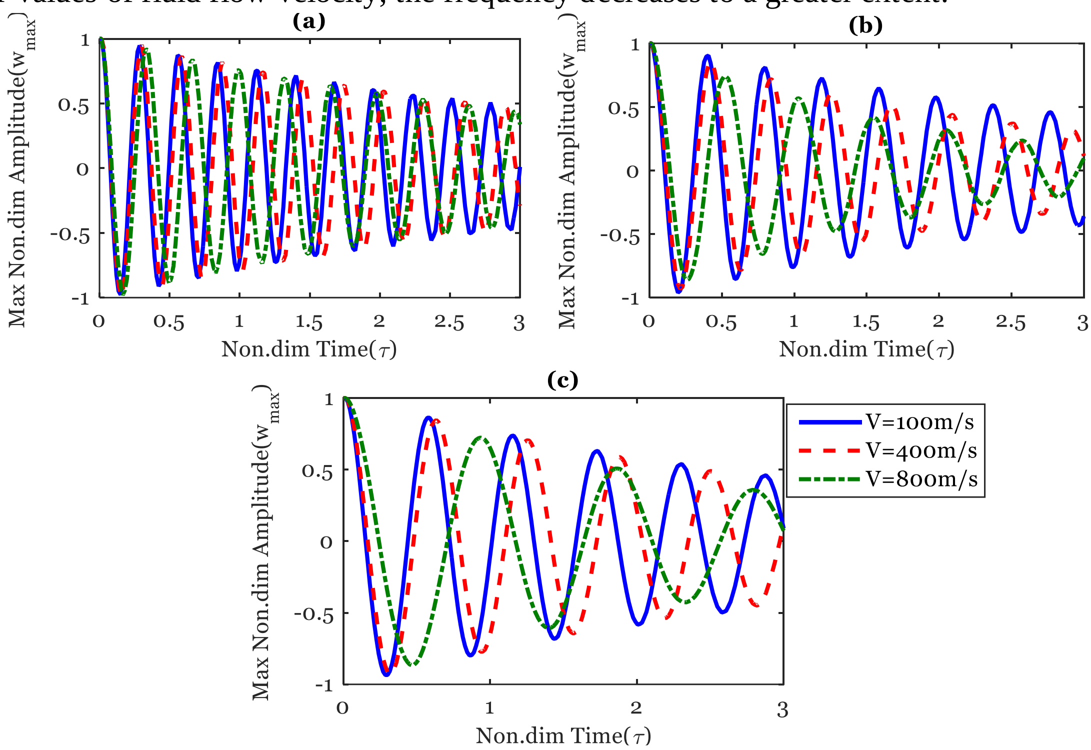

Figure. 6. Effect of fluid flow velocity on the time response of nanotube for a) C-C b) C-SS and c) SS-SS boundary conditions ($\boldsymbol{K = 1\ GPa, \mu = 0.1, \frac{L}{D_o} = 25, c = 10, \mu = 0.1, g = 0.02, \alpha = 0.2, \beta = 0.2}$)

The effect of nonlocal parameter or small scale influence can be analyzed by Fig. 7. It is seen that as the dimensionless nonlocal parameter becomes greater, the frequency decreases and the amplitude is damped to a greater extent.

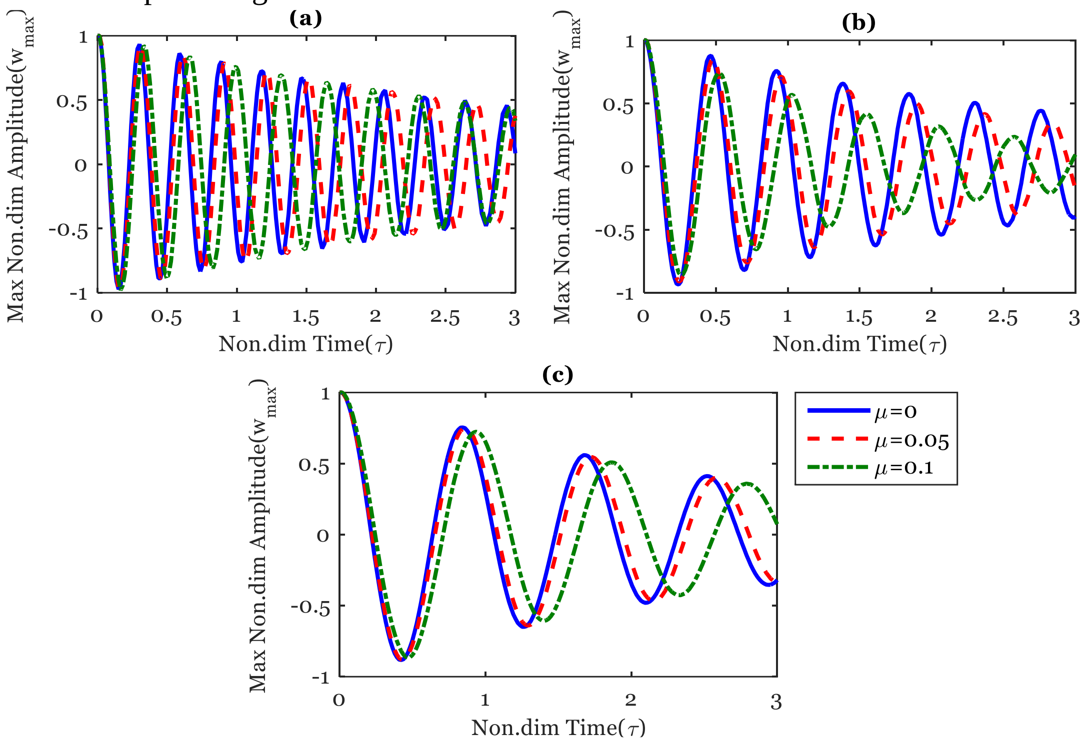

Figure. 7. Effect of nonlocal parameter on the time response of nanotube for a) C-C b) C-SS and c) SS-SS boundary conditions ($\boldsymbol{K = 1\ GPa, \mu = 0.1, \frac{L}{D_o} = 25, c = 10, V = 800\ \frac{m}{s}, g = 0.02, \alpha = 0.2, \beta = 0.2}$)

Fig. 8 indicates the time responses of nanotubes with various L/D_o. It is observed that as L/D_o increases, the damping of system is intensified and its frequency diminishes.

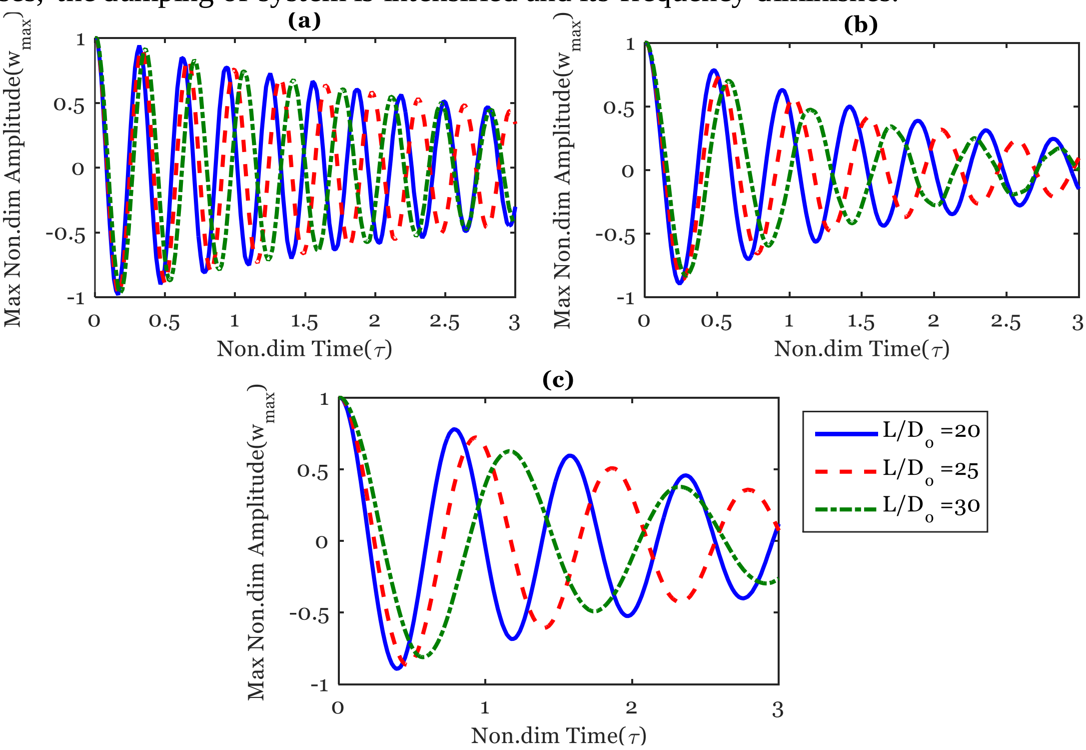

Figure. 8. Effect $\boldsymbol{L/D_o}$ on the time response of nanotube for a) C-C b) C-SS and c) SS-SS boundary conditions ($\boldsymbol{K = 1\ GPa, \mu = 0.1, \mu = 0.1, c = 10, V = 800\ \frac{m}{s}, g = 0.02, \alpha = 0.2, \beta = 0.2}$)

Fig. 9 depicts the effect of foundation's damping coefficient. As expected, increasing this coefficient leads to more damping. Furthermore, the frequency increases with the increase of foundation's damping coefficient.

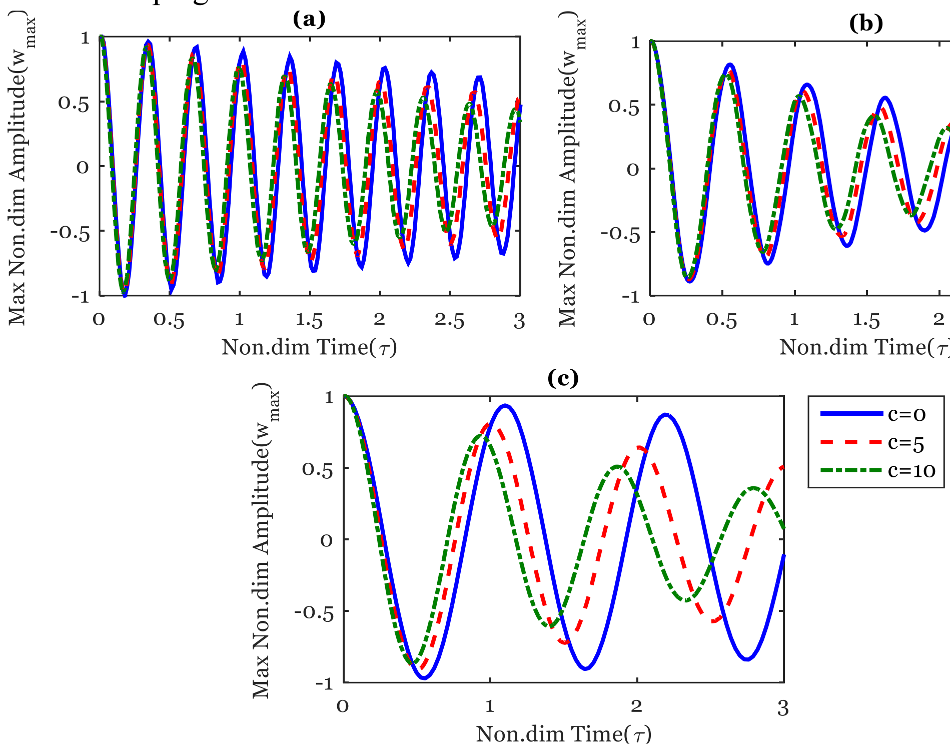

Figure. 9. Effect of foundation's damping coefficient on the time response of nanotube for a) C-C b) C-SS and c) SS-SS boundary conditions ($\boldsymbol{K = 1\ GPa, \mu = 0.1, L/D_o = 25, V = 800\ \frac{m}{s}, g = 0.02, \alpha = 0.2, \beta = 0.2}$)

Finally, the influence of dimensionless viscoelasticity coefficient is studied in Fig. 10. This figure shows that the frequency of nanotube increases as the viscoelasticity coefficient gets larger.

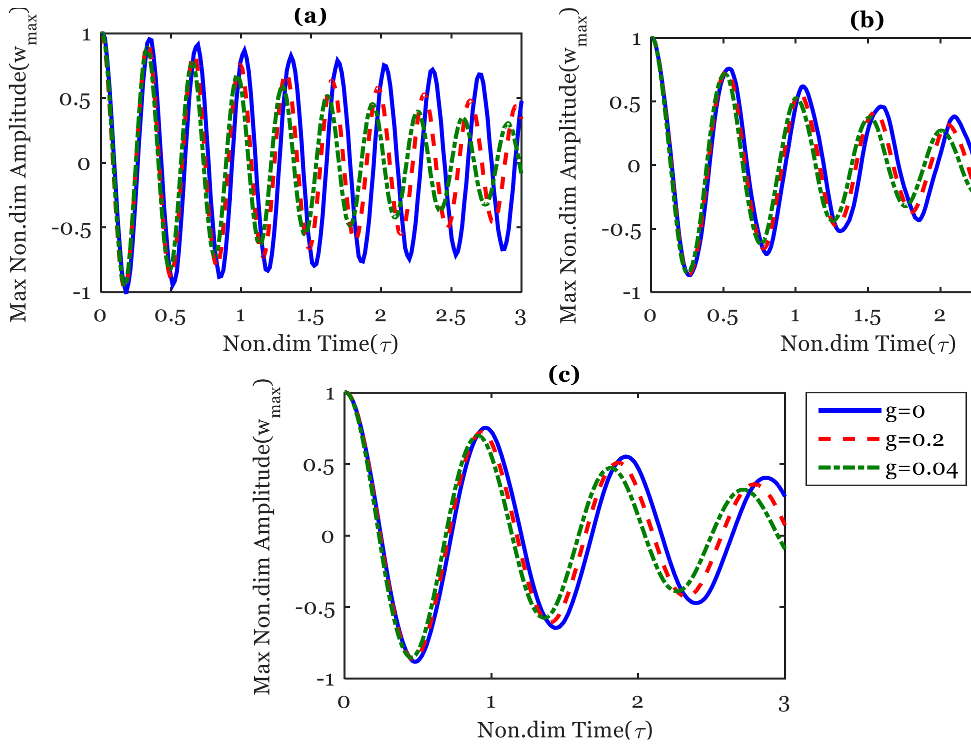

Figure. 10. Effect of viscoelasticity coefficient on the time response of nanotube for a) C-C b) C-SS and c) SS-SS boundary conditions ($\boldsymbol{K = 1\ GPa, \mu = 0.1, \frac{L}{D_o} = 25, V = 800\ \frac{m}{s}, c = 10, \alpha = 0.2, \beta = 0.2}$)

5. Conclusion

Within the framework of fractional calculus, the size-dependent vibrational behavior of viscoelastic conveying fluid carbon nanotubes considering viscoelastic foundation was investigated in this article. The Bernoulli-Euler beam theory, Eringen's nonlocal theory, Kelvin-Voigt model and Hamilton's principle were employed to derive the governing equation which was then solved using two solution approaches. The first approach was based upon the Galerkin method, and in the second approach that was numerical, the GDQ and FD schemes were used. The agreement between the two approaches appears to be sufficient to confirm the validity of the results. The results revealed that as the fractional derivative orders increase, the frequency of system does not change significantly, but the damping of amplitude is intensified. Also, it was concluded that the frequency increases when foundation's spring and damping coefficients become larger. Another finding was that the frequency of system decreases with increasing fluid flow velocity. Moreover, by increasing the fluid flow velocity, the damping of amplitude is intensified. It was also observed that the small scale effect in the nonlocal continuum model make CNTs more flexible.

.

References

[1] Iijima, S. (1991). Helical Microtubes of Graphitic Carbon, *Nature, 354*, 56-58.
[2] Dillon, A. C., Jones, K. M., Bekkedahl, T. A., Klang, C. H., Bethune, D. S., & Heben, M. J. (1997). Storage of Hydrogen in Single-Walled Carbon Nanotubes, *Nature, 386*, 377-379.
[3] Dalton, A. B., Collins, S., Muñoz, E., Razal, J. M., Ebron, V. H., Ferraris, J. P., Coleman, J. N., Kim, B. G., & Baughman, R. H. (2003) Super-Tough Carbon-Nanotube Fibres, *Nature, 423*, 361-368.
[4] Postma, H. W. Ch., Teepen, T., Yao, Z., Grifoni, M., & Dekker, C. (2001) Carbon Nanotube Single-Electron Transistors at Room Temperature, *Science, 293*, 76-79.
[5] Chen, P., Kim, H. S., Kwon, S. M., Yun, Y. S., & Jin, H. J. (2009) Regenerated Bacterial Cellulose/Multi-Walled Carbon Nanotubes Composite Fibers Prepared by Wet-Spinning, *Curr. Appl. Phys., 9*, 96-99.
[6] Guldi, D. M., Rahman, G. M. A., Prato, M., Jux, N., Qin, S., & Ford, W. (2005) Single-Wall Carbon Nanotubes as Integrative Building Blocks for Solar-Energy Conversion, *Angew. Chem., 117*, 2051-2054.
[7] Miaudet, P., Badaire, S., Maugey, M., Derré, A., Pichot, V., Launois, P., Poulin, P., & Zakri, C. (2005). Hot-Drawing of Single and Multiwall Carbon Nanotube Fibers for High Toughness and Alignment, *Nano Lett., 5*, 2212-2215.
[8] Zhang, M., Fang, S., Zakhidov, A. A., Lee, S. B., Aliev, A. E., Williams, C. D., Atkinson, K. R., & Baughman, R. H. (2005) Strong, Transparent, Multifunctional, Carbon Nanotube Sheets, *Science, 309*, 1215-1219.
[9] Nardelli, M. B., & Bernholc, J. (1999) Mechanical Deformations and Coherent Transport in Carbon Nanotubes, *Phys. Rev. B, 60*, R16338-R16341.
[10] Falvo, M. R., Clary, G. J., Taylor, R. M., Chi, V., Brooks, F. P., Washburn, S., & Superfine, R. (1997) Bending and Buckling of Carbon Nanotubes under Large Strain, *Nature, 389*, 582-584.
[11] Gurtin, M. E., & Murdoch, A. I. (1975) A Continuum Theory of Elastic Material Surfaces, *Arch. Rat. Mech. Anal., 57*, 291-323.
[12] Gurtin, M. E., & Murdoch, A. I. (1978) Surface Stress in Solids, *Int. J. Solids Struct., 14*, 431-440.
[13] Gibbs, J. W. (1906) The Scientific Papers of J. Willard Gibbs, Vol. 1. London, Longmans-Green.

[14] Sedighi, H. M., Keivani, M., & Abadyan, M. (2015) Modified continuum model for stability analysis of asymmetric FGM double-sided NEMS: Corrections due to finite conductivity, surface energy and nonlocal effect, *Compos. Part B: Eng.*, *83*, 117–133.
[15] Ansari, R., Mohammadi, V., Faghih Shojaei, M., Gholami, R., & Rouhi, H. (2014) Nonlinear Vibration Analysis of Timoshenko Nanobeams Based on Surface Stress Elasticity Theory, *Eur. J. Mech. A/Solids*, *45*, 143-152.
[16] Rouhi, H., Ansari, R., & Darvizeh, M. (2016) Size-dependent free vibration analysis of nanoshells based on the surface stress elasticity, *Appl. Math. Model.*, *40*, 3128–3140.
[17] Rouhi, H., Ansari, R., & Darvizeh, M. (2016) Analytical treatment of the nonlinear free vibration of cylindrical nanoshells based on a first-order shear deformable continuum model including surface influences, *Acta Mech*., DOI 10.1007/s00707-016-1595-4.
[18] Sedighi, H. M., & Bozorgmehri, A. (2016) Nonlinear vibration and adhesion instability of Casimir-induced nonlocal nanowires with the consideration of surface energy, *J. Brazilian Soc. Mech. Sci. Eng.*, DOI: 10.1007/s40430-016-0530-x.
[19] Rouhi, H., Ansari, R., & Darvizeh, M. (2016). Nonlinear free vibration analysis of cylindrical nanoshells based on the Ru model accounting for surface stress effect, *Int. J. Mech. Sci.*, *113*, 1–9.
[20] Tadi Beni, Y., Koochi, A., Kazemi, A. S., & Abadyan, M. (2012) Modeling the influence of surface effect and molecular force on pull-in voltage of rotational nano–micro mirror using 2-DOF model, *Canadian J. Phys.*, *90*, 963-974.
[21] Ansari, R., Mohammadi, V., Faghih Shojaei, M., Gholami, R., & Sahmani, S. (2014) On the forced vibration analysis of Timoshenko nanobeams based on the surface stress elasticity theory, *Compos. Part B: Eng.*, *60*, 158–166.
[22] Eringen, A. C. (1983). On Differential Equations of Nonlocal Elasticity and Solutions of Screw Dislocation and Surface Waves, *J. Appl. Phys.*, *54*, 4703-4710.
[23] Eringen, A. C. (2002) Nonlocal Continuum Field Theories, Springer, New York.
[24] Yan, J. W., Tong, L. H., Li, C., Zhu, Y., & Wang, Z. W. (2015) Exact solutions of bending deflections for nano-beams and nano-plates based on nonlocal elasticity theory, *Compos. Struct.*, *125*, 304–313.
[25] Zamani Nejad, M., Hadi, A., & Rastgoo, A. (2016) Buckling analysis of arbitrary two-directional functionally graded Euler–Bernoulli nano-beams based on nonlocal elasticity theory, *Int. J. Eng. Sci.*, *103*, 1–10.
[26] Ansari, R., Shahabodini, A., Rouhi, H., & Alipour, A. (2013) Thermal buckling analysis of multi-walled carbon nanotubes through a nonlocal shell theory incorporating interatomic potentials, *J. Therm. Stresses*, *36*, 56–70.
[27] Ghorbanpour Arani, A., & Kolahchi, R. (2014) Exact solution for nonlocal axial buckling of linear carbon nanotube hetero-junctions, *Proc. Inst. Mech. Eng., Part C: J. Mech. Eng. Sci. 228*, 366-377.
[28] Rouhi, H., & Ansari, R. (2012) Nonlocal analytical Flugge shell model for axial buckling of double-walled carbon nanotubes with different end conditions, *NANO*, *7*, 1250018.
[29] Ansari, R., Rouhi, H., & Mirnezhad, M. (2014) A hybrid continuum and molecular mechanics model for the axial buckling of chiral single-walled carbon nanotubes, *Curr. Appl. Phys.*, *14*, 1360-1368.
[30] Farajpour, A., Hairi Yazdi, M. R., Rastgoo, A., Loghmani, M., & Mohammadi, M. (2016) Nonlocal nonlinear plate model for large amplitude vibration of magneto-electro-elastic nanoplates, *Compos. Struct.*, *140*, 323–336.
[31] Ansari, R., Gholami, R., & Rouhi, H. (2015) Size-Dependent Nonlinear Forced Vibration Analysis of Magneto-Electro-Thermo-Elastic Timoshenko Nanobeams Based upon the Nonlocal Elasticity Theory, *Compos. Struct.*, *126*, 216–226.
[32] Demir, Ç., & Civalek, Ö. (2013) Torsional and longitudinal frequency and wave response of microtubules based on the nonlocal continuum and nonlocal discrete models, *Appl. Math. Model.*, *37*, 9355–9367.
[33] Ansari, R., Rouhi, H., & Sahmani, S. (2014) Free Vibration analysis of single- and double-walled carbon nanotubes based on nonlocal elastic shell models, *J. Vib. Control*, *20*, 670-678.
[34] Challamel, N., Picandet, V., Elishakoff, I., Wang, C. M., Collet, B., & Michelitsch, T. (2015) On Nonlocal Computation of Eigenfrequencies of Beams Using Finite Difference and Finite Element Methods, *Int. J. Str. Stab. Dyn.*, *15*, 1540008.
[35] Natsuki, T., Matsuyama, N., & Ni, Q., Q. (2015) Vibration analysis of carbon nanotube-based resonator using nonlocal elasticity theory, *Appl. Phys. A*, *120*, 1309-1313.
[36] Hummer, G., Rasaiah, J. C., & Noworyta, J. P. (2001). Water conduction through the hydrophobic channel of a carbon nanotube, *Nature*, *414*, 188–190.

[37] Ansari, R., Mahmoudinezhad, E., Alipour, A., & Hosseinzadeh, M. (2013). A comprehensive study on the encapsulation of methane in single-walled carbon nanotubes, *J. Comput. Theor. Nanosci., 10*, 2209-2215.
[38] Gao, Y., and Bando, Y. (2002). Nanotechnology: carbon nanothermometer containing gallium, *Nature, 415*, 599.
[39] Foldvari, M., & Bagonluri, M. (2008). Carbon nanotubes as functional excipients for nanomedicines: II. Drug delivery and biocompat-ibility issues, *Nanomed. Nanotechnol. Biol. Med., 4*, 183–200.
[40] Zhang, J., & Meguid, S. A. (2016). Effect of surface energy on the dynamic response and instability of fluid-conveying nanobeams, *Eur. J. Mech. A/Solids, 58*, 1–9.
[41] Ansari, R., Norouzzadeh, A., Gholami, R., Faghih Shojaei, M., & Hosseinzadeh, M. (2014). Size-dependent nonlinear vibration and instability of embedded fluid-conveying SWBNNTs in thermal environment, *Physica E, 61*, 148–157.
[42] Hosseini, M., & Sadeghi-Goughari, M. (2016) Vibration and instability analysis of nanotubes conveying fluid subjected to a longitudinal magnetic field, *Appl. Math. Model., 40*, 2560–2576.
[43] Ansari, R., Gholami, R., Norouzzadeh, A., & Darabi, M. A. (2015) Surface stress effect on the vibration and instability of nanoscale pipes conveying fluid based on a size-dependent Timoshenko beam model, *Acta Mech. Sin., 31*, 708-719.
[44] Ansari, R., Norouzzadeh, A., Gholami, R., Faghih Shojaei, M., & Darabi, M. A. (2016) Geometrically nonlinear free vibration and instability of fluid-conveying nanoscale pipes including surface stress effects, *Microfluidics and Nanofluidics, 20*, 28.
[45] Chang, T. P., 2011, Thermal-Nonlocal Vibration and Instability of Single-Walled Carbon Nanotubes Conveying Fluid, J. Mech., 27, pp. 567-573.
[46] Ansari, R., Faraji Oskouie, M., Sadeghi, F., & Bazdid-Vahdati, M. (2015) Free vibration of fractional viscoelastic Timoshenko nanobeams using the nonlocal elasticity theory, *Physica E, 74*, 318-327.
[47] Faraji Oskouie, M., Ansari, R., & Rouhi, H. (2020) Investigating vibrations of viscoelastic fluid-conveying carbon nanotubes resting on viscoelastic foundation using a nonlocal fractional Timoshenko beam model, *Proc. IMechE Part N: J. Nanomater. Nanoeng. Nanosys.*, DOI: 10.1177/2397791420931701.
[48] Ansari, R., Faraji Oskouie, M., & Gholami, R. (2016) Size-dependent geometrically nonlinear free vibration analysis of fractional viscoelastic nanobeams based on the nonlocal elasticity theory, *Physica E, 75*, 266-271.
[49] Lakes, R. S. (2009). Viscoelastic Materials, Cambridge University Press.
[50] Paidoussis, M. P. (1998) Fluid–Structure Interaction, vol. 1, Academic Press, San Diego.
[51] Hartley, T. T., Lorenzo, C. F., & Killory Qammer, H. (1995). Chaos in a fractional order Chua's system, IEEE Trans. Circuits Sys. I: *Fundamental Theor. Appl., 42*, 485-490.
[52] Shu, C. (2000). Differential Quadrature and Its Application in Engineering, Springer, London.
[53] Liu, F., Meerschaert, M. M., McGough, R. J., Zhuang, P., & Liu, Q. (2013). Numerical methods for solving the multi-term time-fractional wave-diffusion equation, *Fract. Calculus Appl. Anal., 16*, 9-25.
[54] Zhuang, P., & Liu, F. (2007). Finite difference approximation for two-dimensional time fractional diffusion equation, *J. Algor. Comput. Technol., 1*, 1-15.
[55] Ghavanloo, E., Daneshmand, F., & Rafiei, M. (2010). Vibration and instability analysis of carbon nanotubes conveying fluid and resting on a linear viscoelastic Winkler foundation, *Physica E, 42*, 2218-2224.